Research

New Phytologist

Phenotypic plasticity in plant height shaped by interaction between genetic loci and diurnal temperature range

Qi Mu[1], Tingting Guo[1], Xianran Li[1,2] and Jianming Yu[1]

[1]Department of Agronomy, Iowa State University, Ames, IA 50011, USA; [2] Present address: USDA, Agricultural Research Service, Wheat Health, Genetics, and Quality Research Unit, Pullman, WA 99164, USA

Authors for correspondence:
Jianming Yu
Email: jmyu@iastate.edu

Xianran Li
Email: xianran.li@usda.gov

Received: *30 June 2021*
Accepted: *21 November 2021*

New Phytologist (2022) **233:** 1768–1779
doi: 10.1111/nph.17904

Key words: complex trait dissection, diurnal temperature range, genetic effect, growth and development, phenotypic plasticity, plant height, reaction norm.

Summary

- Phenotypic plasticity is observed widely in plants and often studied with reaction norms for adult plant or end-of-season traits. Uncovering genetic, environmental and developmental patterns behind the observed phenotypic variation under natural field conditions is needed.
- Using a sorghum (*Sorghum bicolor*) genetic population evaluated for plant height in seven natural field conditions, we investigated the major pattern that differentiated these environments. We then examined the physiological relevance of the identified environmental index by investigating the developmental trajectory of the population with multistage height measurements in four additional environments and conducting crop growth modelling.
- We found that diurnal temperature range (DTR) during the rapid growth period of sorghum development was an effective environmental index. Three genetic loci (*Dw1*, *Dw3* and *qHT7.1*) were consistently detected for individual environments, reaction-norm parameters across environments and growth-curve parameters through the season. Their genetic effects changed dynamically along the environmental gradient and the developmental stage. A conceptual model with three-dimensional reaction norms was proposed to showcase the interconnecting components: genotype, environment and development.
- Beyond genomic and environmental analyses, further integration of development and physiology at the whole-plant and molecular levels into complex trait dissection would enhance our understanding of mechanisms underlying phenotypic variation.

Introduction

An organism's final phenotypes are determined by genes, environmental factors and the developmental process during which the interaction between genes and environmental factors happens (Scheres & Van Der Putten, 2017). Phenotypic plasticity is the property of a given genotype to produce different phenotypes in response to distinct environmental conditions (Pigliucci, 2001). Phenotypic plasticity in traits such as flowering time, plant height, or grain yield is usually studied by plotting and analysing reaction norm with trait values collected across environments at trait maturity. However, because the final trait has originated from complex processes of growth and development, examining from a developmental perspective is desirable to fully understand the phenotypic plasticity (Pigliucci *et al.*, 1996, 1997; Sultan, 2000; Bahuguna & Jagadish, 2015). The ontogeny trajectory is vital to understanding phenotypic plasticity during development (Pigliucci *et al.*, 1996; Wright & Mcconnaughay, 2002). One can view the plasticity's expression over time from an ontogeny trajectory perspective, including variation in rates and timing of phenotypic response (Sultan, 2004).

Knowing environmental cues that trigger phenotypic plasticity is essential for studying adaptability under climate change (Bonamour *et al.*, 2019). Environmental stimuli at a particular stage of growth can be critical for a trait's final phenotype (Wright & Mcconnaughay, 2002; Bahuguna & Jagadish, 2015; Abley *et al.*, 2016). Identifying the critical crop growth period sensitive to environmental stimuli could facilitate crop improvements. Studies in phenotypic plasticity have expanded from a species' adaptation fitness (Bradshaw, 2006; Nicotra *et al.*, 2010; Josephs, 2018) to genetic and molecular control for within species diversity (Quint *et al.*, 2016; Kusmec *et al.*, 2017; Laitinen & Nikoloski, 2019; Li *et al.*, 2021). Although challenging for natural field conditions, identifying critical environmental cues and understanding the genetic and functional mechanisms of plants' responses to the environmental stimuli can advance our understanding of phenotypic plasticity and increase predictive capability for future performance.

Plant height is an agronomically important trait regulated by genetic factors and also subject to environmental changes (Ballaré *et al.*, 1987; Erwin & Heins, 1995; Rajapakse *et al.*, 1999; Shimizu & Heins, 2000; Wallace *et al.*, 2016; Perrier *et al.*, 2017; Kronenberg *et al.*, 2021). In particular, the diurnal temperature range (DTR) (Easterling *et al.*, 1997), or the difference between day and night temperature (also referred as DIF), has been shown to control stem elongation (Erwin *et al.*, 1989;

Myster & Moe, 1995). However, the effect of DTR on plant height under natural field conditions, particularly in combination with genetic analysis, has not been reported. During the Green Revolution, plant height in wheat and rice was reduced to increase resistance to lodging and harvestable yield (Hedden, 2003). Conversely, taller plant height is desired for biomass production in energy grass species (Fernandez *et al.*, 2009). Sorghum plant height can range from 0.6 to 4.5 m (Quinby & Karper, 1954). Tall alleles are partially dominant and present in most landraces worldwide, while the dwarf alleles were identified and introduced to the US sorghum breeding systems (Morris *et al.*, 2013). Among four major sorghum *dwarfing* loci (*Dw1–Dw4*) regulating stem internode length (Quinby & Karper, 1954), *Dw3* encodes a P-glycoprotein involved in polar auxin transport (Multani *et al.*, 2003); *Dw1* is a positive regulator of the brassinosteroid signalling (Hilley *et al.*, 2016; Yamaguchi *et al.*, 2016; Hirano *et al.*, 2017); and *Dw2* encodes an AGCVIII kinase modulating endomembrane function and cell division (Hilley *et al.*, 2017; Oliver *et al.*, 2021). Our previous work on sorghum plant height identified another plant height locus, *qHT7.1*, localised near the *Dw3* region on chromosome 7 that showed a strong effect on plant height (Li *et al.*, 2015). In the previous work (Li *et al.*, 2015), phenotypic plasticity was not investigated due to the small set of environments.

Recently, we developed the Critical Environmental Regressor through Informed Search (CERIS) algorithm and established a CERIS-Joint Genomic Regression Analysis (CERIS-JGRA) framework to dissect the phenotypic variation of complex traits observed in natural field conditions by identifying and leveraging explicit environmental indices (Li *et al.*, 2018, 2021; Guo *et al.*, 2020). These studies aimed at bridging physiological understanding of environmental conditions on phenotypic traits with genetic dissection of phenotypic variation across environments into multiple reaction norms at single gene or multilocus levels. However, the biological relevance of the environmental indices and dynamic genetic effects across environments have not been adequately investigated and empirically demonstrated, even though they generally agreed with the understanding in crop physiology.

To add a developmental perspective to reveal the interconnected genetic and environmental origins of phenotypic variation observed in natural field conditions, and to better understand phenotypic plasticity for improved genomic prediction under different environments, we conducted the current study. We found that phenotypic variation observed in plant height of a sorghum genetic population can be effectively quantified with an environmental index: DTR during the rapid growth period. We demonstrated the physiological meaning of the identified environmental index by analysing and modelling the height developmental trajectories. In addition, quantitative trait locus (QTL) analyses identified the same set of genetic loci underlying the final plant height across and within environments, the height progression during development within individual environments (i.e. different stages and logistic growth-curve parameters), and the plant height phenotypic plasticity across environments (i.e. reaction-norm parameters).

Materials and Methods

Population and phenotyping

The sorghum (*Sorghum bicolor*) 237 recombinant inbred lines (RILs) population was derived from a cross between Tx430 and P898012. Randomised complete block design with two replications was used in seven environments to obtain initial phenotypic data: Manhattan, Kansas, USA in 2011 and 2012 (KS11 and KS12), two winter nurseries in 2011, 2012, and one summer season in 2014 in Puerto Rico (PR11, PR12, and PR14S), and Ames, Iowa in 2013 and 2014 (IA13 and IA14). Single-row plots with 12.5-feet length and 30-inch row spacing were used. The final plant height was measured at maturity from the soil surface to the panicle apex. The environmental mean of plant height was calculated as the average plant height of the entire population in each environment.

Empirical validation and multistage measurement experiment was conducted with the same experimental design in four additional environments: Ames, Iowa in 2015, 2016, 2018, and 2019 (IA15, IA16, IA18 and IA19). Plant height was measured five to nine times through each growing season. For IA15, plant height was measured using the plot canopy height until flag leaf fully expanded, then flag leaf height of a representative plant from each plot was used until flowering, and finally the panicle apex height measurements were used. For IA16, IA18 and IA19, plant height was measured using the plot canopy height until flowering (50% shedding pollen), then using the panicle apex height of a representative plant from each plot. Flowering time was recorded as the number of days after planting when half of the plot was shedding pollen (Li *et al.*, 2018).

R package (R Core Team, 2021) LME4 was used to calculate the best linear unbiased estimator (BLUE) values of plant height and flowering time for each genotype at each environment and growth stages. The plant height phenotype of individual k in jth replication at environment i was modelled as:

$$Y_{ijk} = u + E_i + B_{(i)j} + G_k + \mathrm{EG}_{ik} + e_{ijk}$$

where u is the mean of the population; E_i is the effect of environment; $B_{(i)j}$ is the effect of the replication nested in environment; G_k is the effect of genotype; EG_{ik} is the interaction between environment and genotype; and e_{ijk} is the error. Variance component analysis was conducted using the VCA package in R.

Identifying the environmental index

Daily maximum and minimum air temperature ($T_{\max}$ and $T_{\min}$ in Fahrenheit) were retrieved from the Global Historical Climatology Network (GHCN) database at National Oceanic and Atmospheric Administration (NOAA)'s National Centers for Environmental Information (NCEI) (https://www.ncdc.noaa.gov/). Up to three weather stations within 50 miles of the field sites were considered, and average values were used. Day length (DL) was obtained by applying the daylength function in the geosphere package in R. Daily growing degree days (GDD) were calculated as $((T_{\max} + T_{\min})/2 - T_{\mathrm{base}})$,

with T_{max} greater than 100°F adjusted to 100°F, T_{min} lower than 50°F adjusted to 50°F, and T_{base} set to 50°F. The photothermal time (PTT) was calculated as GDD × DL. The daily DTR was calculated as $T_{max} - T_{min}$, without any adjustment applied to T_{max} or T_{min}, such as GDD.

Average GDD, DL, PTT, and DTR values with different starting days with a window size from 5 to 25 d during the growing season were obtained for each environment. Then the obtained environmental parameter values at each specific growth window (expressed as days after planting) were correlated with the environmental means (average plant height of the entire population at each environment). The combination of environmental parameter and growth window with the most significant correlation, support from nearby windows and meaningful biological relevance was chosen as the environmental index.

The joint-regression analysis was first conducted by regressing the plant height values of individual RILs against environmental means (Li *et al.*, 2018; Guo *et al.*, 2020). Reaction norms of individual genotypes were generated. The identified environmental index was used as the explanatory variable to replace the environmental mean in the second joint-regression analysis. Environmental mean and environmental index were centred by the average values before joint-regression analysis to obtain two sets of reaction-norm parameters, intercept and slope. These average values were added back during plotting.

Modelling the growth trajectory

Logistic regression was fitted separately to the measured plant height data over time for each genotype at each validation environment (IA15, IA16, IA18 and IA19), following the method in Bustos-Korts *et al.*, 2019.

$$y_t = \frac{A}{1 + e^{-k(t-t_m)}} + \epsilon_t \qquad \text{Eqn 1}$$

In Eqn (1), y_t is the value of plant height for one genotype at t d after planting (DAP), A is the final plant height at the end of the season (asymptote), k is the initial relative growth rate, t_m is the day at which plant height reached maximum growth rate (inflection point), and ϵ_t is the residual. The maximum growth rate was when the second derivative equals zero, which is $(1/4)kA$. The *nls* function of the STATS package in R was used. The daily growth rate over time was computed based on the first derivative of the fitted logistic growth curve for each genotype.

Fitted logistic growth curves for environmental means were constructed based on the population means of the measured data across time. Additional information about simulating growth trajectories for the first set of seven environments is presented in Methods S1.

Genetic mapping, functional polymorphisms and haplotype analysis

The genetic map was built with 1462 SNP markers from 8960 SNPs generated by genotyping by sequencing (Li *et al.*, 2015). Composite interval mapping was conducted with WINDOWS QTL CARTOGRAPHER 2.5 (Wang *et al.*, 2012). QTL mapping was performed for each individual environment, developmental stage and model-derived parameter. Intercept and slope were obtained by regressing phenotypes of each RIL on environmental index using R. These intercept and slope values were then treated as phenotypes to map QTL for these two reaction-norm parameters. Maximum growth rate and inflection date from the logistic growth curve were used to map the developmental trajectory-related QTL.

Dw1 (*Sobic.009G229800*) and *Dw3* (*Sobic.007G163800*) genes are located in the QTL intervals. Following the previous publication (Li *et al.*, 2018), 15.8 Gb whole-genome Illumina paired-end reads of Tx430 (SRR2759161) and 59.8 Gb Illumina paired-end reads of P898012 (SRR4028763 and SRR4028764) were used to verify the segregation of reported functional polymorphisms.

GBS markers at *Dw1*, *Dw3* and *qHT7.1* QTL peak regions were used as the genotypes for each RIL. In total 202 RILs had genotype information and were homozygous at all three QTL regions for subsequent analysis. The RILs were grouped into four haplotype groups based on the number of dominant alleles carried at *Dw1*, *Dw3* and *qHT7.1*, which are the height-increasing, wild-type alleles. Group 0 represented the RILs carrying all recessive (height-decreasing) alleles at these three QTLs, while group 3 represented the RILs carrying all dominant alleles at these three QTLs. Group 1 represented having one dominant allele from either *Dw1*, *Dw3* or *qHT7.1* and group 2 represented having two dominant alleles at two of the three QTL. Reaction norms, logistic growth curves and daily growth rate curves were visualised and analysed by grouping RILs based on these four haplotype groups.

Performance prediction and validation

Performance prediction with JGRA was first conducted within seven initial environments, and the model built with the entire seven environments and the predictions were validated for four empirical validation environments (Li *et al.*, 2018, 2021; Guo *et al.*, 2020). For the scenario of tested genotype in untested environments, leave-one-environment-out cross-validations were conducted to examine the predictive ability. In each run, six environments were used to build the model to predict each genotype's plant height in the remaining one environment. The reaction-norm parameters (slope and intercept) were obtained by regressing individual genotype's plant height values across six environments on the environmental index. The environmental index value of the untested environment was then factored into the regression model to obtain the predicted performance. Predictive ability was calculated as the correlation coefficient between the observed and predicted plant height values.

Additional information about performance prediction for two other scenarios is presented in the Methods S1.

For empirical validation, the values for DTR_{40-53} were obtained for IA15, IA16, IA18 and IA19 from environmental data. Plant height of each genotype was predicted based on the

reaction norms of the training model established using the data from the seven initial environments and the $DTR_{40–53}$ values from the validation environments.

Results

Sorghum final plant height plasticity under natural field conditions

We measured the final plant height of a sorghum population containing 237 RILs from a bi-parental cross between Tx430 and P898012 in seven natural field environments (Fig. 1a; Supporting Information Table S1). Within each environment, plant height between two replicates was highly correlated (Fig. S1). The generally low correlations between plant height and previously characterised flowering time in this population (Fig. 1b) indicated that there were different mechanisms underlying these two traits (Li *et al.*, 2018). Variance component analysis attributed 66.6% of the plant height variation to genotypes, 13.3% of the variation to the environment, and 9.3% to G × E (Table S2). The environmental mean – average plant height of the entire population at each environment – ranged from 125.5 cm to 188.2 cm (Table S1). For each RIL, the ratio between the tallest observation and the shortest observation across environments reached up to 2.5, with an average ratio of 1.6 ± 0.2 (Fig. 1c; Table S3). The plant height variation did not show a discernible pattern when the reaction norm was plotted with environments arranged based on latitude (Fig. 1c).

To unravel the pattern underneath the complex trait variation, we first applied joint-regression analysis (Finlay & Wilkinson, 1963; Eberhart & Russell, 1966) using the environmental mean as explanatory variable to model phenotypic variation (Figs 1c,d, S2). A general scale change pattern was observed (linear model average R^2 value of 0.65; Table S4). More than 70% of RILs had slope values significantly different from zero (Figs 1d, S3a; Table S4). However, this approach could not explain why this population behaved similarly in two distantly located environments, such as PR12 and IA14, but less similarly at the same location in 2 years consecutively, KS11 and KS12.

DTR from early season as the environmental index

We applied CERIS to identify the combination of environmental parameter and growth window that is strongly correlated with the environmental mean. After testing DL, GDD, photothermal time (PTT), and DTR, we found that DTR best differentiated the environments to be selected as the environmental index (Fig. S4). Specifically, the DTR value at the period of 40–53 DAP, or $DTR_{40–53}$, had the strongest correlation ($r = -0.995$, $P = 2.9 \times 10^{-6}$) with the environmental mean (Figs 2b,c, S4). For every degree increased in $DTR_{40–53}$, the average plant height decreased by 4.2 cm (Fig. 2c).

Research from earlier studies under controlled, constant growing conditions showed that DTR regulated plant morphological traits, particularly plant height (Erwin *et al.*, 1989; Myster & Moe, 1995). With varied daily conditions from natural fields, our current analysis established the connection between DTR and sorghum plant height and narrowed down the effect of DTR to a particular growth period, which was best represented by the 40–53 DAP growth window and supported by the surrounding windows (Fig. 2a,b). Checking flowering records (the majority of RILs flowered after 61 DAP across all seven environments) verified that this 40–53 DAP growth period generally corresponded to the vegetative growth stage.

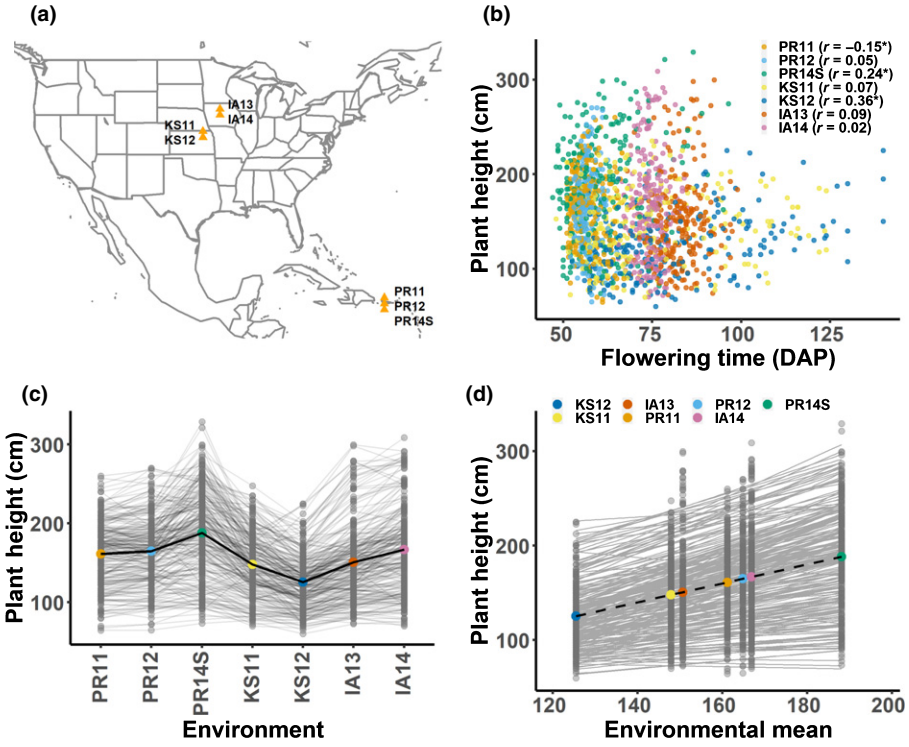

Fig. 1 Plant height variation and phenotypic plasticity of a sorghum genetic population. (a) Seven natural field environments from three locations in 4 yr. (b) Low correlations between plant height and flowering time in this population. Correlation coefficients and significance levels are labelled in parenthesis for each environment. *, $P < 0.05$. (c) Plant height variation does not follow the latitude gradient. Lines are the connected heights of individual recombinant inbred lines (RILs) across environments. (d) Reaction norms of individual RILs fitted with the joint-regression analysis using environmental mean. Dots are observed values and lines are regression-fitted values. Environmental mean (coloured dots in c and d), average plant height of the population at each environment.

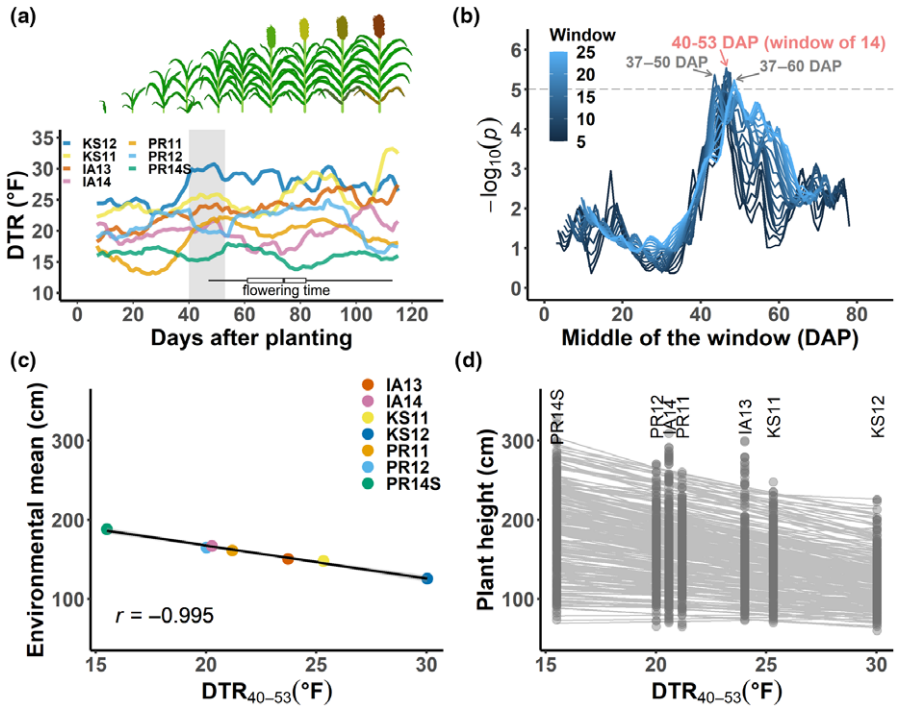

Fig. 2 Identifying an environmental index for sorghum plant height variation. (a) Daily diurnal temperature range (DTR) profile of seven environments during the growing season. (b) Significance of correlation between environmental mean and DTR across growing season. DTR within the 40–53 d after planting (DAP) window, or $DTR_{40–53}$, had the most significant correlation with environmental mean. Window: number of days included in the search. (c) The strong correlation between $DTR_{40–53}$ and the environmental mean of plant height. (d) Regression-fitted reaction norm using $DTR_{40–53}$ as the explanatory variable for individual RILs. Dots are observed values and lines are regression-fitted values.

Using the $DTR_{40–53}$ as the explanatory variable to model plant height captured the general trend of trait variation across environments (average R^2 value of 0.64; Table S5). The slopes ranged from −9.8 to 1.3 with an average of −4.2 (Fig. S3b; Table S5). In total, 69% of RILs had slope values significantly different from zero (Table S5). Through the identified $DTR_{40–53}$ to quantify the environmental gradient, regression-fitted reaction norms were obtained with two sets of parameters (intercept and slope) (Fig. 2d).

Dynamic effects of genetic loci along the environmental gradient

We conducted genetic mapping in the seven environments separately with the final plant height first. Although a few minor QTLs were detected in certain environments, three QTLs were consistently detected: two on chromosome 7 and one on chromosome 9 (Fig. S5a; Table S6). These QTLs were co-localised with the previously identified plant height regulating loci *qHT7.1*, *Dw3* and *Dw1* (Multani *et al.*, 2003; Li *et al.*, 2015; Hilley *et al.*, 2016; Yamaguchi *et al.*, 2016). *Dw3* and *Dw1* were cloned as the ABC1 auxin transporter (Multani *et al.*, 2003) and the positive regulator in the brassinosteroid signalling (Hirano *et al.*, 2017), respectively, while the gene underlying *qHT7.1* has not been identified. No QTLs corresponding to *Dw2* or *Dw4* were detected in this population (Table S6).

We then conducted mapping with two reaction-norm parameters: intercept and slope. (Fig. 3a). Intercept quantified the average performance for each RIL across all environments, and the slope quantified the plasticity along the environmental gradient. The same set of QTLs was detected for both reaction-norm parameters as for individual environments, indicating that the genetic loci *qHT7.1*, *Dw3* and *Dw1* controlled phenotypic plasticity by their differential response to the environmental input quantified by the DTR gradient (Fig. 3a). To examine each individual locus further, we obtained the genetic effects of *qHT7.1*, *Dw3* and *Dw1* from the mapping results of the individual environment analysis. The size of genetic effects for *qHT7.1* and *Dw3* varied across environments, but generally decreased along the identified $DTR_{40–53}$ gradient, showing differential allelic sensitivity (Figs 3b, S5b). The less pronounced effect changes in *Dw1* (Fig. 3b) agreed with the reduced significance of its genetic effect on slope (Fig. 3a).

Aligning our current analyses and previous studies (Multani *et al.*, 2003; Li *et al.*, 2015; Hilley *et al.*, 2016; Yamaguchi *et al.*, 2016) indicated that the dominant alleles of *qHT7.1*, *Dw3* and *Dw1* were responsible for taller plant height and a higher plasticity level. To reveal the allelic effect on phenotypic plasticity, we grouped the RILs based on the number of dominant alleles (Fig. 3c) and surveyed the distributions of intercept and slope (Fig. S5c,d). The individuals carrying all three dominant alleles (haplotype group 3) had the highest plant height values and the steepest slopes (Figs 3c, S5c,d). This finding is consistent with the findings that natural variants of *Dw1* and *Dw3* are recessive, loss-of-function alleles (Fig. 3d). The wild-type dominant alleles maintained the normal signalling pathways, which interacted with environmental cues during development and led to varied final plant height across diverse environments. By contrast, the signal transduction pathways were disrupted by the loss-of-function alleles, resulting in less sensitivity to environmental cues and shorter final plant height.

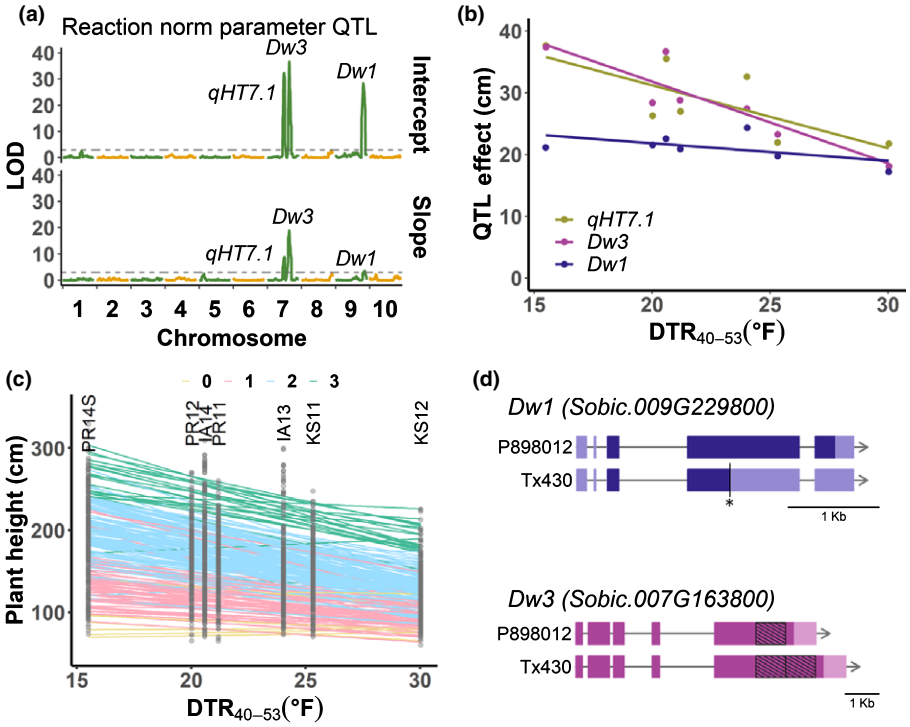

Fig. 3 Identifying genetic loci underlying phenotypic plasticity in sorghum plant height. (a) Quantitative trait locus (QTL) mapping of reaction-norm parameters (intercept and slope) showed *Dw1*, *Dw3* and *qHT7.1* controlled plant height plasticity. (b) Effects of *Dw1*, *Dw3* and *qHT7.1* from mapping within individual environments changed dynamically across the gradient of the diurnal temperature range at the period of 40–53 d after planting ($DTR_{40–53}$). (c) Reaction norms of plant height on $DTR_{40–53}$, colour-coding based on four haplotype groups. Groups 0 to 3 show the number of dominant alleles carried at *Dw1*, *Dw3* and *qHT7.1*. (d) Known functional polymorphisms between two alleles in *Dw1* and *Dw3* genes. Recessive alleles resulted from premature stop codon (asterisk/vertical line) in *Dw1* and an 882-bp tandem repeat (dashed black box) in *Dw3*. Dark colours: coding sequence; light colours: 5′ untranslated region (UTR) or 3′UTR regions.

Multistage plant height measurements confirmed DTR and the critical window

To elucidate the physiological meaning of the identified environmental index, $DTR_{40–53}$, we measured plant height across developmental stages in four new environments (Fig. 4a; Table S7). The final plant height values for the population varied only slightly for these four new environments (Tables S1, S7). Checking DTR profiles across the growing season indicated that, despite varying to a higher degree before and after the period 40–53 DAP, the DTR values were very similar during this period across the four environments (Fig. 4b), matching our expectation based on the environmental index.

Using multistage measurement data, we modelled the growth trajectory of each individual by a logistic growth curve (Archontoulis & Miguez, 2015) (Figs 4b, S6). Indeed, the 40–53 DAP growth window aligned well with the rapid growth period during plant development (Fig. 4b). To further uncover the relationship between $DTR_{40–53}$ and growth trajectory, we estimated the daily growth rate at these four environments by obtaining the first derivative of the logistic fitted curves. The inflection point, where the maximum growth rate is reached, landed within the 40–53 growth window for all four environments (Fig. 4c). The inflection point in the logistic growth curve represented the end of the exponential growth phase and the beginning of the asymptotic phase (Fig. 4c) (Zhao *et al.*, 2004). This result validated that this 40–53 DAP growth window generally covered the rapid growth period during sorghum development, which was also the most influential phase determining the final plant height. Checking the inflection date, the date when the maximum growth rate was observed, showed that the majority of the RILs had their inflection dates during or near the 40–53 DAP window (Fig. 4d).

In addition, we conducted simulations for growth trajectories for the previous seven environments, in which only the final plant height was measured (Figs S7, S8). Similar to the four validation environments with multistage measurements, the 40–53 DAP growth window generally aligned with the maximum growth period (inflection dates) (Fig. S7).

Dynamic effects of genetic loci during development

To understand the genetic mechanisms of plant height progression during development, we conducted genetic mapping at different time points across growth in individual environments (Figs 5a, S9). Three QTLs, *qHT7.1*, *Dw3* and *Dw1*, were detected in all four environments. These QTLs were detected as early as 39 to 46 DAP in IA16, with the highly significant peaks identified after 53 DAP in all four environments (Fig. S9). The effect sizes of *Dw1*, *Dw3* and *qHT7.1* started to deviate from zero and gradually showed more substantial effects during the 40–53 DAP growth window and eventually plateaued *c.* 80 DAP (Fig. 5b). Consistent results were obtained for the three other environments (Fig. S10a).

We further investigated the genetic contributions across development by mapping with the two parameters related to the logistic growth-curve inflection point: maximum growth rate and inflection date. All three QTLs (*qHT7.1, Dw3* and *Dw1*) were found regulating maximum growth rate and inflection date (Figs 5c, S11). *Dw3* contributed the most in regulating the maximum growth rate, while *Dw1* and *qHT7.1* contributed more to inflection date regulation. To reveal the developmental pattern governed jointly by these three loci, we used the same haplotype grouping based on the number of dominant alleles carried at *qHT7.1, Dw3* and *Dw1* as for the previous analysis. As expected,

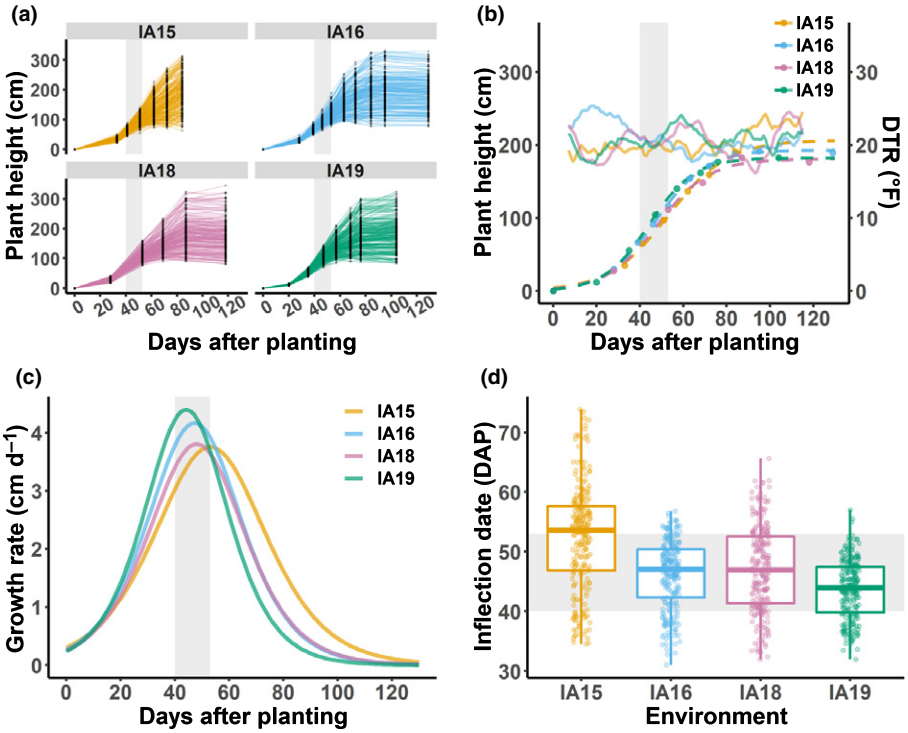

Fig. 4 Multistage measurement to show that the 40–53 d after planting (DAP) window overlapped with the rapid growth period during sorghum development. (a) Growth curve of each recombinant inbred line (RIL) in four new environments. Plant height measurements are shown in black dots. (b) Logistic regressions of the average plant height (environmental mean) across RILs during development and the diurnal temperature range (DTR) variation during the growing season in four environments. Dots: average plant height across RILs at measurement dates. Dashed lines: logistic regression of plant height. Solid lines: DTR. (c) The average daily growth rate of the entire RIL population. (d) Distribution of the inflection date, the day of maximum growth rate, from logistic regression across all RILs. Grey zone shows the 40–53 DAP window, which overlapped with the period of maximum growth rate in (c) and (d). In boxplots, horizontal lines are medians, ranges are from 25 to 75 percentile, and dots are actual values.

the final plant height was the tallest for the group with all three dominant alleles, group 3 (Figs 5d, S10b). While sharing a generally similar growth pattern, these four groups showed some difference in growth rate and/or inflection date. The shortest group had the lowest growth rate and earliest inflection date, and the growth rate and/or inflection date increased as the number of dominant alleles increased (Figs 5d, S10). Conversely, even with the differences among the haplotypes, the 40–53 DAP window generally covered the maximum growth period for all four haplotype groups (Figs 5d, S10).

Performance prediction facilitated by environmental index and genomic prediction

To assess utility of the combined analysis framework of environmental index and genomic prediction, we first conducted leave-one-environment-out cross-validation within the seven environments. The predictive ability (i.e. the correlation between predicted and observed values) within each environment ranged from 0.76 to 0.95, with the overall predictive ability of 0.89 achieved across all environments (Fig. S12a). We also applied the CERIS-JGRA approach to two other scenarios (Li *et al.*, 2018, 2021; Guo *et al.*, 2020). For predicting untested genotypes in tested environments, the overall predictive ability was 0.69 (Fig. S12b). For the most challenging scenario, predicting untested genotypes in untested environments (leave-one-environment-and-one-tenth-genotypes-out cross-validation), the overall predictive ability was 0.65 (Fig. S12c).

We then conducted empirical validations with data from four new environments. The plant height predicted was strongly correlated with the observed plant height, with an overall predictive ability of 0.91 (Fig. S12d). Within each environment, the predictive ability ranged from 0.88 to 0.96. The overall ratio between the observed and predicted was 1.09, indicating that the prediction was also largely on target (Table S8). Future validation experiments may consider other locations that better capture the range of the environmental index ($DTR_{40–53}$) values. Additional methodology exploration may be carried out with the data (Table S9).

Developmental dimension of reaction norms and phenotypic complexity

To encapsulate our enriched understanding, we created three-dimensional reaction norms to show the developmental dimension of reaction norms and phenotypic complexity to highlight the connections among gene/genetics, environment, and physiology using findings from the current study as an example (Fig. 6). For phenotypic variation observed as the end-of-season measurements or at trait maturity for a labile trait, patterns extracted at the differentiating environmental index and the individual organism levels can be seen as the outcome of the developmental process, as modelled here with logistic growth curves for plant height, during which the gene–environmental interplay carries out. Reaction norm and phenotypic plasticity of individual organisms depicted using data from a given time including the typically studied, end-of-season timepoint are snapshots of the entire live and interacting processes. Reaction norms at the various genetic effect levels at a given time or across the season can then be deduced from those of individual organisms with the known genotype, haplotype, allele, sequence and functional polymorphism information.

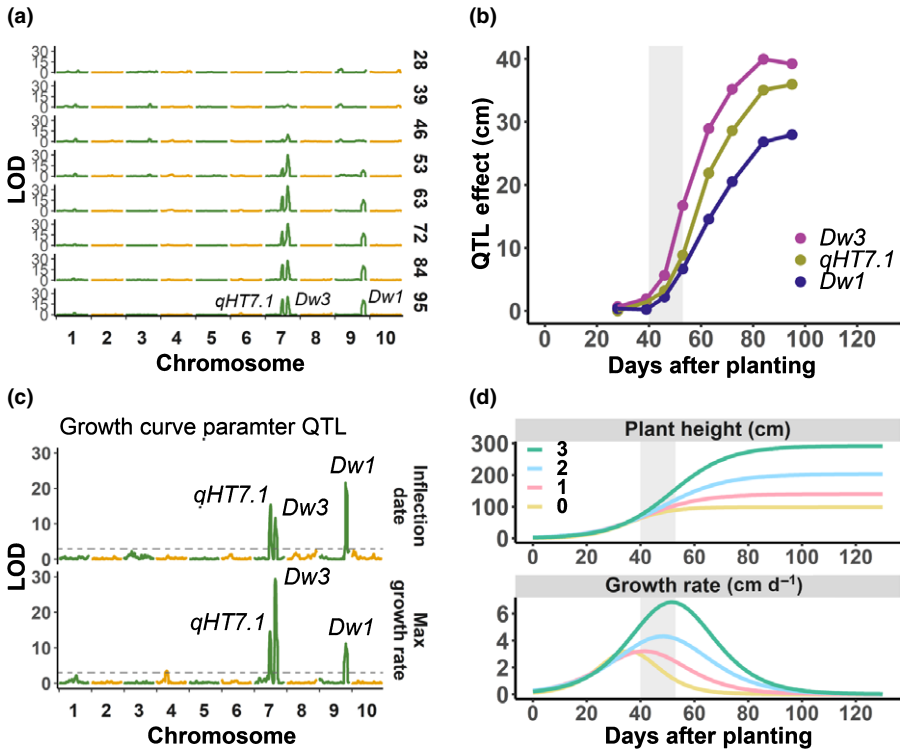

Fig. 5 Three quantitative trait loci (QTLs) (*Dw1*, *Dw3 and qHT7.1*) controlled sorghum plant height during development (example from IA16). (a) Progression of plant height QTL peaks along development. Numbers on the right axis show the days after planting of plant height measurements. (b) Dynamic change of QTL effects of *Dw1*, *Dw3* and *qHT7.1* across development. (c) Composite interval mapping showed these three QTLs controlled inflection date and maximum growth rate. (d) Fitted logistic regressions (upper) and derived growth rate (lower) on the average plant height grouped by number of dominant alleles carried at the three QTL. Legend (groups 0–3) shows the number of dominant alleles carried at *Dw1*, *Dw3* and *qHT7.1*. Grey zone shows the 40–53 growth window.

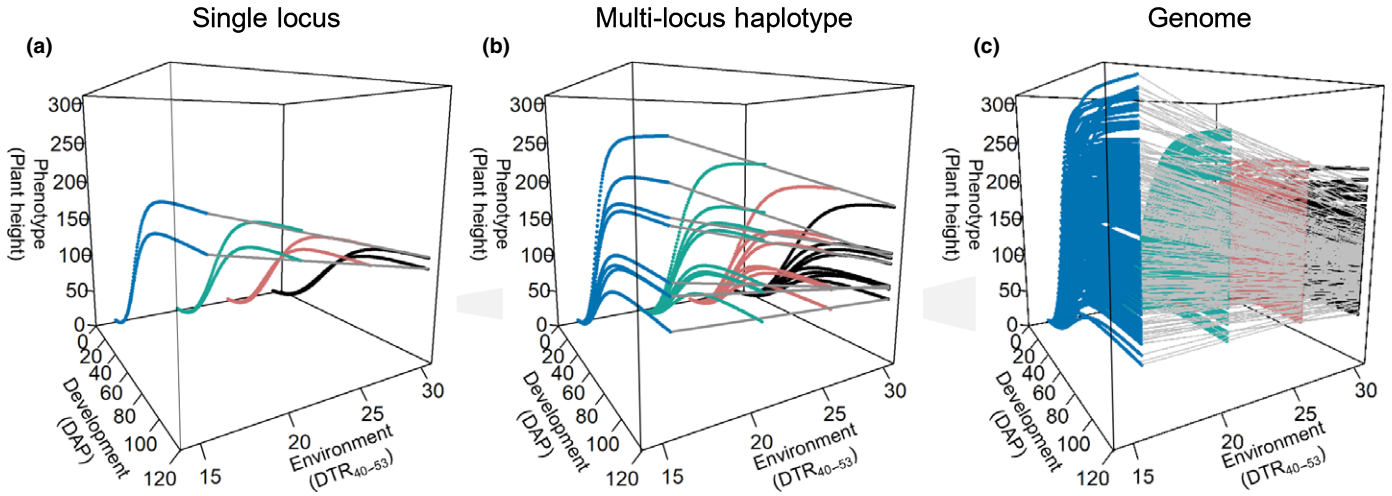

Fig. 6 A conceptual model to show the joint determination of phenotype by genotype, environment and development using three-dimensional (3D) reaction norms with growth trajectories at multiple genetics levels with varied environmental inputs. (a) 3D reaction norms at the single locus level to changes in diurnal temperature range (DTR) across development at different days after planting (DAP). Two alleles of the gene *Dw3* represent two homozygous genotypes. (b) 3D reaction norms at the multilocus haplotype level. The $2^3 = 8$ haplotypes represent eight homozygous genotypes across three loci (*Dw1*, *Dw3* and *qHT7.1*). (c) 3D reaction norms at the genome level observed as individual organisms. The typical 2D reaction norms for final plant height are shown with grey lines on the front surface.

Discussion

Uncovering the mechanisms underlying the phenotypic variation of complex traits is important research in biology, evolution, agriculture and medical science (Mackay *et al.*, 2009; Boyle *et al.*, 2017). We presented findings from dissecting phenotypic plasticity under natural field conditions with a developmental perspective in addition to environmental and genetic analyses. While it is recognised that incorporating developmental process is important to fully understand the complex plasticity and phenotypic variation (Wright & Mcconnaughay, 2002), many large-scale field-based studies in plants have been primarily focused on the phenotypes measured at a single time point at the trait maturity (Kusmec *et al.*, 2017; Li *et al.*, 2018, 2021; Millet *et al.*, 2019; Guo *et al.*, 2020). Genetic mapping on trait development and functional mapping through growth trajectories were investigated (Zhao *et al.*, 2004; Wu & Lin, 2006; Moore *et al.*, 2013; Miao *et al.*, 2020), providing insights into the genetic regulation

for trait development. With the advancement of high-throughput phenotyping, multistage trait measurements are becoming more accessible for large-scale field-based genetics studies (Pugh *et al.*, 2018; Anderson *et al.*, 2020; Wang *et al.*, 2020). At the same time, how to best leverage the technology and crop growth models to enrich our biological understanding is also important. Our study investigated plant height plasticity by identifying an environmental index, validated the physiological relevance of this index with a developmental trajectory approach and unveiled the genetic and environmental determinants underlying plant height during development and across environments.

Identifying the environmental parameter under natural field conditions is essential for understanding the mechanism for phenotypic plasticity. Earlier studies have shown the difference between day and night temperatures regulating plant height under controlled glasshouse or growth chamber conditions (Erwin *et al.*, 1989; Moe, 1990; Myster & Moe, 1995; Stavang *et al.*, 2005; Yang *et al.*, 2013), in which ornamental and horticultural species were the primary targets, and that its effect on stem elongation was through promoting cell elongation (Erwin & Heins, 1995). However, to the best of our knowledge, no study was reported about DTR effect under natural field environments. We found that the DTR under natural environments was negatively correlated with the final plant height in sorghum, different from the positive relationship reported in some earlier studies under controlled conditions. Among possible explanations, constant DTR settings were generally applied throughout the entire growth in controlled environments, while fluctuating DTR occurred in field conditions. Stem elongation was sensitive to a short period of temperature drop during the last part of the night or the first period of the day (Myster & Moe, 1995), during which the minimum temperature usually occurs under natural conditions. Second, higher night temperature over day temperature (negative DTR) could suppress stem elongation leading to short plant height, which is usually tested in controlled conditions (Moe, 1990; Erwin *et al.*, 1993; Xiong *et al.*, 2011). Different ranges of tested DTR can lead to different relationships with the stem length (Davies *et al.*, 2002; Schouten *et al.*, 2002; Sunoj *et al.*, 2016). Our validation experiments confirmed the DTR's role in controlling sorghum plant height under natural field conditions. This finding may also be incorporated into crop modelling to enhance the phenotypic prediction for field crops (Hammer *et al.*, 2010).

Plant height is arguably an ideal trait to validate the critical growth window. As a labile trait, its trajectory can be easily tracked, unlike other labile traits such as flowering time, for which intensive and destructive dissection of floral initiation is needed. Utilising the logistic regression for ontogenetic analysis, we connected the plant height plasticity with growth rate and DTR under natural field conditions, providing support to the ontogenetic perspective of whole organism-environment interactions (Pigliucci, 1998). Developmental reaction norm describes the integration of three aspects of phenotypic plasticity: genetic, environmental, and developmental (Pigliucci *et al.*, 1996). We showed that the growth trajectory parameter (maximum growth rate) was different when the same individual was grown under different natural environments, but the inflection date generally occurred during the identified critical growth window. We empirically validated that DTR's window is physiologically relevant because it was aligned with the most rapid growth period. While different environmental inputs are not possible to manipulate under natural field conditions, the design of future research under controlled and dynamically programmable conditions would benefit from the current findings.

The genetic control of sorghum final plant height, plant height phenotypic plasticity and plant height developmental trajectories were unified in this study. Three final plant height QTLs (*Dw1*, *Dw3* and *qHT7.1*) were consistently identified for all these analyses. Specifically, phenotypic plasticity in sorghum final height exhibited differential sensitivity: QTL effects being significant but with varying effect sizes across environments (Des Marais *et al.*, 2013). In addition, our QTL analyses suggested that (1) the *Dw1*, *Dw3* and *qHT7.1* controlled final plant height during growth by regulating the maximum growth rate and the timing to reach the maximum growth rate; (2) the genetic effect sizes for these loci emerged and increased exponentially during the 40–53 DAP growth window; and (3) the input level of environmental stimuli (i.e. DTR), which sorghum plants experienced during this critical growth period, influenced the trait expression, leading to varied final plant height in distinct environments. Conversely, in addition to the general pattern captured by the environmental index and consistently detected QTLs across environments and through reaction-norm parameters, unique environmental conditions will alter the trait expression at different environments through other genetic loci. Their effects would generally not be detected by mapping the reaction-norm parameters, which capture the general pattern across environments.

Continued development and application of high-throughput phenotyping and envirotyping (i.e. extensive environmental characterisation), and enhanced analytics and modelling would greatly complement the current capacity in genotyping, sequencing, gene cloning and 'omics technologies to further integrate genetics, genomics, genetic diversity and physiology to build a better understanding of phenotypic plasticity of complex traits. Improved understanding of the genetic, environmental and developmental mechanisms underlying complex traits can not only provide guidelines on germplasm enhancement, cultivar placement, environmental classification and agronomic management, but also help to translate discoveries in basic science (e.g. functional genomics, regulatory mechanisms, and genome editing) into sustainable agriculture production practice.

Acknowledgements

This work was supported by the Agriculture and Food Research Initiative competitive grant (2017-67007-25942 and 2021-67013-33833) and the Hatch project (1021013) from the USDA National Institute of Food and Agriculture, the Iowa State University Raymond F. Baker Center for Plant Breeding, and the Iowa State University Plant Sciences Institute.

Author contributions

JY and XL conceived the original research plans and supervised the experiments; QM and XL performed experiments; XL, TG and QM developed the code for data analysis; QM analysed the data and wrote the article with contributions of all the authors. JY and XL agree to serve as the authors responsible for contact and ensure communication.

ORCID

Tingting Guo https://orcid.org/0000-0002-6647-6998
Xianran Li https://orcid.org/0000-0002-4252-6911
Qi Mu https://orcid.org/0000-0001-9093-9123
Jianming Yu https://orcid.org/0000-0001-5326-3099

Data availability

All data are included in the manuscript and/or its Supporting Information.

References

Abley K, Locke JCW, Leyser HMO. 2016. Developmental mechanisms underlying variable, invariant and plastic phenotypes. *Annals of Botany* **117**: 733–748.

Anderson SL, Murray SC, Chen Y, Malambo L, Chang A, Popescu S, Cope D, Jung J. 2020. Unoccupied aerial system enabled functional modeling of maize height reveals dynamic expression of loci. *Plant Direct* **4**: e00223.

Archontoulis SV, Miguez FE. 2015. Nonlinear regression models and applications in agricultural research. *Agronomy Journal* **107**: 786–798.

Bahuguna RN, Jagadish KSV. 2015. Temperature regulation of plant phenological development. *Environmental and Experimental Botany* **111**: 83–90.

Ballaré CL, Sánchez RA, Scopel AL, Casal JJ, Ghersa CM. 1987. Early detection of neighbour plants by phytochrome perception of spectral changes in reflected sunlight. *Plant, Cell & Environment* **10**: 551–557.

Bonamour S, Chevin L-M, Charmantier A, Teplitsky C. 2019. Phenotypic plasticity in response to climate change: the importance of cue variation. *Philosophical Transactions of the Royal Society of London. Series B: Biological Sciences* **374**: 20180178.

Boyle EA, Li YI, Pritchard JK. 2017. An expanded view of complex traits: from polygenic to omnigenic. *Cell* **169**: 1177–1186.

Bradshaw AD. 2006. Unravelling phenotypic plasticity–why should we bother? *New Phytologist* **170**: 644–648.

Bustos-Korts D, Boer MP, Malosetti M, Chapman S, Chenu K, Zheng B, van Eeuwijk FA. 2019. Combining crop growth modeling and statistical genetic modeling to evaluate phenotyping strategies. *Frontiers in Plant Science* **10**: 1491.

Davies LJ, Brooking IR, Catley JL, Halligan EA. 2002. Effects of day/night temperature differential and irradiance on the flower stem quality of *Sandersonia aurantiaca*. *Scientia Horticulturae* **95**: 85–98.

Des Marais DL, Hernandez KM, Juenger TE. 2013. Genotype-by-environment interaction and plasticity: exploring genomic responses of plants to the abiotic environment. *Annual Review of Ecology, Evolution, and Systematics* **44**: 5–29.

Easterling DR, Horton B, Jones PD, Peterson TC, Karl TR, Parker DE, Salinger MJ, Razuvayev V, Plummer N, Jamason P *et al.* 1997. Maximum and minimum temperature trends for the globe. *Science* **277**: 364–367.

Eberhart SA, Russell WA. 1966. Stability Parameters for comparing varieties 1. *Crop Science* **6**: 36–40.

Erwin JE, Heins RD, Karlsson MG. 1989. Thermomorphogenesis in *Lilium longiflorum*. *American Journal of Botany* **76**: 47–52.

Erwin JE, Heins RD. 1995. Thermomorphogenic responses in stem and leaf development. *HortScience* **30**: 940–949.

Erwin JE, Pierson G, Strefeler M, Heins R. 1993. Temperature manipulation of vegetable stem elongation and flowering. *Minnesota Flower Growers Bulletin* **42**: 6–10.

Fernandez MGS, Becraft PW, Yin Y, Lübberstedt T. 2009. From dwarves to giants? Plant height manipulation for biomass yield. *Trends in Plant Science* **14**: 454–461.

Finlay KW, Wilkinson GN. 1963. The analysis of adaptation in a plant-breeding programme. *Australian Journal of Agricultural Research* **14**: 742–754.

Guo T, Mu Q, Wang J, Vanous AE, Onogi A, Iwata H, Li X, Yu J. 2020. Dynamic effects of interacting genes underlying rice flowering-time phenotypic plasticity and global adaptation. *Genome Research* **30**: 673–683.

Hammer GL, van Oosterom E, McLean G, Chapman SC, Broad I, Harland P, Muchow RC. 2010. Adapting APSIM to model the physiology and genetics of complex adaptive traits in field crops. *Journal of Experimental Botany* **61**: 2185–2202.

Hedden P. 2003. The genes of the Green Revolution. *Trends in Genetics* **19**: 5–9.

Hilley J, Truong S, Olson S, Morishige D, Mullet J. 2016. Identification of Dw1, a regulator of sorghum stem internode length. *PLoS ONE* **11**: e0151271.

Hilley JL, Weers BD, Truong SK, Mccormick RF, Ashley J, Mckinley BA, Morishige DT, Mullet JE. 2017. Sorghum Dw2 encodes a protein kinase regulator of stem internode length. *Scientific Reports* **7**: 4616.

Hirano KO, Kawamura M, Araki-Nakamura S, Fujimoto H, Ohmae-Shinohara K, Yamaguchi M, Fujii A, Sasaki H, Kasuga S, Sazuka T. 2017. Sorghum DW1 positively regulates brassinosteroid signaling by inhibiting the nuclear localization of BRASSINOSTEROID INSENSITIVE 2. *Scientific Reports* **7**: 126.

Josephs EB. 2018. Determining the evolutionary forces shaping $G \times E$. *New Phytologist* **219**: 31–36.

Kronenberg L, Yates S, Boer MP, Kirchgessner N, Walter A, Hund A. 2021. Temperature response of wheat affects final height and the timing of stem elongation under field conditions. *Journal of Experimental Botany* **72**: 700–717.

Kusmec A, Srinivasan S, Nettleton D, Schnable PS. 2017. Distinct genetic architectures for phenotype means and plasticities in *Zea mays*. *Nature Plants* **3**: 715–723.

Laitinen RAE, Nikoloski Z. 2019. Genetic basis of plasticity in plants. *Journal of Experimental Botany* **70**: 739–745.

Li X, Guo T, Mu Q, Li X, Yu J. 2018. Genomic and environmental determinants and their interplay underlying phenotypic plasticity. *Proceedings of the National Academy of Sciences, USA* **115**: 6679–6684.

Li X, Guo T, Wang J, Bekele WA, Sukumaran S, Vanous AE, McNellie JP, Tibbs-Cortes LE, Lopes MS, Lamkey KR *et al.* 2021. An integrated framework reinstating the environmental dimension for GWAS and genomic selection in crops. *Molecular Plant* **14**: 874–887.

Li X, Li X, Fridman E, Tesso TT, Yu J. 2015. Dissecting repulsion linkage in the dwarfing gene Dw3 region for sorghum plant height provides insights into heterosis. *Proceedings of the National Academy of Sciences, USA* **112**: 11823–11828.

Mackay TFC, Stone EA, Ayroles JF. 2009. The genetics of quantitative traits: challenges and prospects. *Nature Reviews Genetics* **10**: 565–577.

Miao C, Xu Y, Liu S, Schnable PS, Schnable JC. 2020. Increased power and accuracy of causal locus identification in time series genome-wide association in sorghum. *Plant Physiology* **183**: 1898–1909.

Millet EJ, Kruijer W, Coupel-Ledru A, Prado SA, Cabrera-Bosquet L, Lacube S, Charcosset A, Welcker C, van Eeuwijk F, Tardieu F. 2019. Genomic prediction of maize yield across European environmental conditions. *Nature Genetics* **51**: 952–956.

Moe R. 1990. Effect of day and night temperature alternations and of plant growth regulators on stem elongation and flowering of the long-day plant Campanula isophylla Moretti. *Scientia Horticulturae* **43**: 291–305.

Moore CR, Johnson LS, Kwak I-Y, Livny M, Broman KW, Spalding EP. 2013. High-throughput computer vision introduces the time axis to a quantitative trait map of a plant growth response. *Genetics* **195**: 1077–1086.

Morris GP, Ramu P, Deshpande SP, Hash CT, Shah T, Upadhyaya HD, Riera-Lizarazu O, Brown PJ, Acharya CB, Mitchell SE *et al.* 2013. Population

genomic and genome-wide association studies of agroclimatic traits in sorghum. *Proceedings of the National Academy of Sciences, USA* **110**: 453–458.

Multani DS, Briggs SP, Chamberlin MA, Blakeslee JJ, Murphy AS, Johal GS. 2003. Loss of an MDR transporter in compact stalks of maize *br2* and sorghum *dw3* mutants. *Science* **302**: 81–84.

Myster J, Moe R. 1995. Effect of diurnal temperature alternations on plant morphology in some greenhouse crops-a mini review. *Scientia Horticulturae* **62**: 205–215.

Nicotra AB, Atkin OK, Bonser SP, Davidson AM, Finnegan EJ, Mathesius U, Poot P, Purugganan MD, Richards CL, Valladares F *et al.* 2010. Plant phenotypic plasticity in a changing climate. *Trends in Plant Science* **15**: 684–692.

Oliver J, Fan M, Mckinley B, Zemelis-durfee S, Brandizzi F. 2021. The AGCVIII kinase Dw2 modulates cell proliferation, endomembrane trafficking, and MLG/xylan cell wall localization in elongating stem internodes of *Sorghum bicolor*. *The Plant Journal* **105**: 1053–1071.

Perrier L, Rouan L, Jaffuel S, Clément-vidal A, Roques S, Soutiras A, Baptiste C, Bastianelli D, Fabre D, Dubois C. 2017. Plasticity of sorghum stem biomass accumulation in response to water deficit: a multiscale analysis from internode tissue to plant level. *Frontiers in Plant Science* **8**: 1–14.

Pigliucci M. 1998. Developmental phenotypic plasticity: where internal programming meets the external environment. *Current Opinion in Plant Biology* **1**: 87–91.

Pigliucci M. 2001. *Phenotypic plasticity: beyond nature and nurture*. Baltimore, MD, USA: John Hopkins University Press.

Pigliucci M, Diiorio P, Schlichting CD. 1997. Phenotypic plasticity of growth trajectories in two species of Lobelia in response to nutrient availability. *Journal of Ecology* **85**: 265.

Pigliucci M, Schlichting CD, Jones CS, Schwenk K. 1996. Developmental reaction norms: the interactions among allometry, ontogeny and plasticity. *Plant Species Biology* **11**: 69–85.

Pugh NA, Horne DW, Murray SC, Carvalho G, Malambo L, Jung J, Chang A, Maeda M, Popescu S, Chu T *et al.* 2018. Temporal estimates of crop growth in sorghum and maize breeding enabled by unmanned aerial systems. *The Plant Phenome Journal* **1**: 1–10.

Quinby JR, Karper RE. 1954. Inheritance of height in Sorghum. *Agronomy Journal* **46**: 211–216.

Quint M, Delker C, Franklin KA, Wigge PA, Halliday KJ, Van Zanten M. 2016. Molecular and genetic control of plant thermomorphogenesis. *Nature Plants* **2**: 1–9.

R Core Team. 2021. *R: a language and environment for statistical computing*. Vienna, Austria: R Foundation for Statistical Computing. [WWW document] URL https://www.R-project.org/ [accessed 26 October 2021].

Rajapakse NC, Young RE, McMahon MJ, Oi R. 1999. Plant height control by photoselective filters: current status and future prospects. *Horttechnology* **9**: 618–624.

Scheres B, Van Der Putten WH. 2017. The plant perceptron connects environment to development. *Nature* **543**: 337–345.

Schouten RE, Carvalho SMP, Heuvelink E, Van Kooten O. 2002. Modelling of temperature-controlled internode elongation applied to Chrysanthemum. *Annals of Botany* **90**: 353–359.

Shimizu H, Heins RD. 2000. Photoperiod and the difference between day and night temperature influence stem elongation kinetics in *Verbena bonariensis*. *Journal of the American Society for Horticultural Science* **125**: 576–580.

Stavang JA, Lindga B, Erntsen A, Lid SE, Moe R, Olsen JE. 2005. Thermoperiodic stem elongation involves transcriptional regulation of gibberellin deactivation in pea. *Plant Physiology* **138**: 2344–2353.

Sultan SE. 2000. Phenotypic plasticity for plant development, function and life history. *Trends in Plant Science* **5**: 537–542.

Sultan SE. 2004. Promising directions in plant phenotypic plasticity. *Perspectives in Plant Ecology, Evolution and Systematics* **6**: 227–233.

Sunoj VSJ, Shroyer KJ, Jagadish SVK, Prasad PVV. 2016. Diurnal temperature amplitude alters physiological and growth response of maize (*Zea mays* L.) during the vegetative stage. *Environmental and Experimental Botany* **130**: 113–121.

Wallace JG, Zhang X, Beyene Y, Semagn K, Olsen M, Prasanna BM, Buckler ES. 2016. Genome-wide association for plant height and flowering time across 15 tropical maize populations under managed drought stress and well-watered conditions in Sub-Saharan Africa. *Crop Science* **2378**: 2365–2378.

Wang R, Qiu Y, Zhou Y, Liang Z, Schnable JC. 2020. A high-throughput phenotyping pipeline for image processing and functional growth curve analysis. *Plant Phenomics* **2020**: 7481687.

Wang S, Basten CJ, Zeng ZB. 2012. *Windows Qtl Cartographer 2.5_011*. Raleigh, NC, USA: North Carolina State University.

Wright SD, Mcconnaughay KDM. 2002. Interpreting phenotypic plasticity: the importance of ontogeny. *Plant Species Biology* **17**: 119–131.

Wu R, Lin M. 2006. Functional mapping—how to map and study the genetic architecture of dynamic complex traits. *Nature Reviews Genetics* **7**: 229–237.

Xiong J, Patil GG, Moe R, Torre S. 2011. Effects of diurnal temperature alternations and light quality on growth, morphogenesis and carbohydrate content of *Cucumis sativus* L. *Scientia Horticulturae* **128**: 54–60.

Yamaguchi M, Fujimoto H, Hirano K, Araki-nakamura S. 2016. Sorghum Dw1, an agronomically important gene for lodging resistance, encodes a novel protein involved in cell proliferation. *Scientific Reports* **6**: 28366.

Yang F, Liu F, Rowland G. 2013. Effects of diurnal temperature range and seasonal temperature pattern on the agronomic traits of fibre flax (*Linum usitatissimum* L.). *Canadian Journal of Plant Science* **93**: 1249–1255.

Zhao W, Zhu J, Gallo-meagher M, Wu R. 2004. A unified statistical model for functional mapping of environment-dependent genetic expression and genotype x environment interactions for ontogenetic development. *Genetics* **168**: 1751–1762.

Supporting Information

Additional Supporting Information may be found online in the Supporting Information section at the end of the article.

Fig. S1 Plant height comparisons between two replications at each environment.

Fig. S2 Reaction norms across seven environments and joint-regression analysis of plant height using environmental mean.

Fig. S3 Slope distribution across all recombinant inbred lines.

Fig. S4 Environmental parameters and their correlations at different growth windows with environmental mean at seven environments.

Fig. S5 Genetic control of plant height phenotypic plasticity.

Fig. S6 Logistic regression for all recombinant inbred lines in four Iowa validation environments.

Fig. S7 Growth-curve simulation in seven environments.

Fig. S8 Comparison of growth curves in four Iowa validation environments and simulation for seven environments.

Fig. S9 Quantitative trait locus mapping across developmental stages in four Iowa validation environments.

Fig. S10 Quantitative trait locus effect, growth curves and growth rate of genotypes across developmental stages in four Iowa validation environments.

Fig. S11 Quantitative trait locus mapping of logistic regression parameters: maximum growth rate and inflection date in four Iowa validation environments.

Fig. S12 CERIS-JGRA plant height performance prediction with reaction-norm parameters and genomic data.

Methods S1 Simulation of growth curves in seven environments and performance prediction.

Table S1 Planting date, location and average phenotypes in each of the 11 environments.

Table S2 ANOVA and variance component for plant height across seven environments.

Table S3 Plant height BLUE values across 237 recombinant inbred lines in seven environments.

Table S4 Statistics for joint-regression analysis with environmental mean for 237 RILs.

Table S5 Statistics for joint-regression analysis with environmental index DTR_{40-53} for 237 recombinant inbred lines.

Table S6 Quantitative trait locus detected for plant height in seven environments.

Table S7 Planting date, measurement dates and average plant height in four Iowa validation environments.

Table S8 Empirical validation for plant height predictions in four Iowa validation environments.

Table S9 Genotype, phenotype and environmental data of the study.

Please note: Wiley Blackwell are not responsible for the content or functionality of any Supporting Information supplied by the authors. Any queries (other than missing material) should be directed to the *New Phytologist* Central Office.